

Widths of \bar{K} -nuclear deeply bound states in a dynamical model

J. Mareš ^a, E. Friedman ^b, A. Gal ^b

^a*Nuclear Physics Institute, 25068 Řež, Czech Republic*

^b*Racah Institute of Physics, The Hebrew University, Jerusalem 91904, Israel*

Abstract

The relativistic mean field (RMF) model is applied to a system of nucleons and a \bar{K} meson, interacting via scalar and vector boson fields. The model incorporates the standard RMF phenomenology for bound nucleons and, for the \bar{K} meson, it relates to low-energy $\bar{K}N$ and K^- atom phenomenology. Deeply bound \bar{K} nuclear states are generated dynamically across the periodic table and are exhibited for ^{12}C and ^{16}O over a wide range of binding energies. Substantial polarization of the core nucleus is found for these light nuclei. Absorption modes are also included dynamically, considering explicitly both the resulting compressed nuclear density and the reduced phase space for \bar{K} absorption from deeply bound states. The behavior of the calculated width as function of the \bar{K} binding energy is studied in order to explore limits on the possible existence of narrow \bar{K} nuclear states.

PACS: 13.75.Jz, 25.80.Nv, 36.10.Gv

Keywords: \bar{K} nuclear interaction, \bar{K} nuclear deeply bound states

Corresponding author: Avraham Gal, avragal@vms.huji.ac.il

tel: +972 2 658 4930, fax: +972 2 561 1519

July 26, 2018

I. INTRODUCTION

The $\bar{K}N$ interaction near threshold is strongly attractive, in agreement with the existence of the unstable bound state $\Lambda(1405)$ below the K^-p threshold. The \bar{K} -nucleus interaction is also strongly attractive, as derived from the strong-interaction shifts and widths in kaonic-atom levels across the periodic table [1]. It is not established yet how strong the \bar{K} -nucleus potential is: ‘deep’ (150-200 MeV [2,3]) or relatively ‘shallow’ (50-60 MeV [4,5])? Is it possible to bind *strongly* \bar{K} mesons in nuclei and are such potentially deep bound states sufficiently narrow to allow observation and identification? These issues have received considerable phenomenological and theoretical attention recently [4–8], and some experimental evidence for candidate states in the (K_{stop}^-, n) and (K_{stop}^-, p) reactions on ${}^4\text{He}$ (KEK-PS E471, [9,10] respectively) and in the (K^-, n) in-flight reaction on ${}^{16}\text{O}$ (BNL-AGS, parasite E930 [11]) has been presented very recently. New experiments have been approved at KEK, using (K^-, N) reactions to search for \bar{K} nuclear bound states [12]. (K^-, π^-) reactions [13] were also suggested in this context.

A prime concern in searching for \bar{K} nuclear bound states is the anticipated large width due to pionic conversion modes on a single nucleon:

$$\bar{K}N \rightarrow \pi\Sigma, \pi\Lambda \quad (\sim 80\%) , \quad (1)$$

with thresholds about 100 MeV and 180 MeV, respectively, below the $\bar{K}N$ total mass, and also due to non-pionic multi-nucleon absorption modes, say

$$\bar{K}NN \rightarrow YN \quad (\sim 20\%) , \quad (2)$$

with thresholds about $m_\pi = 140$ MeV lower than the single-nucleon thresholds. The branching ratios in parentheses are known from bubble-chamber experiments [14].

The aim of the present work is to study *dynamical* effects for \bar{K} nuclear states in the range of binding energy $B_K \sim 100 - 200$ MeV [9–11] and in particular the width anticipated for such deeply bound states. The relatively shallow chirally-motivated \bar{K} -nucleus potentials [4,5] which followed the microscopic construction by Ramos and Oset [15] are of no use in this context, since they cannot yield binding energy greater than the potential depth of about 50 MeV. One must therefore depart from the microscopic approach in favor of a more phenomenologically inclined model which is constrained by data other than two-body $\bar{K}N$ observables. The theoretical framework here adopted is the relativistic mean field (RMF) model for a system of nucleons and one \bar{K} meson interacting through the exchange of scalar (σ) and vector (ω) boson fields which are treated in the mean-field approximation. By allowing the \bar{K} to polarize the nucleons, and vice versa, this dynamical calculation is made self consistent. \bar{K} absorption modes are included within a $t\rho$ optical-model approach, where the density ρ plays a dynamical role, and the constant t which is constrained near threshold by K^- -atom data follows the phase-space reduction in reactions Eqs. (1,2) for a deeply bound \bar{K} . A wide range of binding energies may be explored in the RMF calculation simply by scanning over the coupling constants of the \bar{K} meson to the σ and ω boson fields. Detailed calculations were done by us across the periodic table. In this Letter we demonstrate the essential points and conclusions for ${}^{12}\text{C}$ and ${}^{16}\text{O}$ where the dynamical polarization effects are extremely important for the energies of the \bar{K} bound states as well as for their widths.

Akaishi et al. [7,8] too have found large polarization effects in lighter nuclei using few-body variational techniques. The RMF is a systematic approach used across the periodic table beyond the very light elements explored by other techniques, and it can be used also to study multi- \bar{K} configurations and to explore the \bar{K} condensation limit [16,17]. Similar RMF calculations have been recently reported for \bar{N} states in nuclei [18,19].

II. METHODOLOGY

In the calculations described below, the standard RMF Lagrangian \mathcal{L}_N with the linear (L) parameterization of Horowitz and Serot [20] as well as the nonlinear (NL) parameterization due to Sharma et al. [21] are used for the description of the nucleonic sector. The (anti)kaon interaction with the nuclear medium is incorporated by adding to \mathcal{L}_N the Lagrangian density \mathcal{L}_K [16,17]:

$$\mathcal{L}_K = \mathcal{D}_\mu^* \bar{K} \mathcal{D}^\mu K - m_K^2 \bar{K} K - g_{\sigma K} m_K \sigma \bar{K} K . \quad (3)$$

The covariant derivative $\mathcal{D}_\mu = \partial_\mu + ig_{\omega K} \omega_\mu$ describes the coupling of the (anti)kaon to the vector meson ω . The vector field ω is then associated with a conserved current. The coupling of the (anti)kaon to the isovector ρ meson is here excluded due to considering $N = Z$ nuclear cores in this initial report.

Whereas adding \mathcal{L}_K to the original Lagrangian \mathcal{L}_N does not affect the form of the corresponding Dirac equation for nucleons, the presence of \bar{K} leads to additional source terms in the equations of motion for the meson fields σ and ω_0 to which the \bar{K} couples:

$$(-\Delta + m_\sigma^2) \sigma = -g_{\sigma N} \rho_S - g_{\sigma K} m_K \bar{K} K + (-g_2 \sigma^2 - g_3 \sigma^3) , \quad (4)$$

$$(-\Delta + m_\omega^2) \omega_0 = +g_{\omega N} \rho_V - 2g_{\omega K} (\omega_K + g_{\omega K} \omega_0) \bar{K} K , \quad (5)$$

where ω_K is the \bar{K} energy in the nuclear medium:

$$\omega_K = \sqrt{m_K^2 + g_{\sigma K} m_K \sigma + p_K^2} - g_{\omega K} \omega_0 ,$$

and ρ_S and ρ_V denote the nuclear scalar and vector densities, respectively. Adding \bar{K} to the nuclear system affects the scalar and vector potentials which enter the Dirac equation for nucleons. This leads to the rearrangement, or polarization of the nuclear core in the presence of \bar{K} .

In order to preserve the connection to previous studies of kaonic atoms, the Klein Gordon (KG) equation of motion for the \bar{K} is written in the form [5]:

$$[\Delta - 2\mu(B + V_{\text{opt}} + V_c) + (V_c + B)^2] \bar{K} = 0 \quad (\hbar = c = 1) . \quad (6)$$

Here, V_c denotes the static Coulomb potential for the K^- , μ is the \bar{K} -nucleus reduced mass and $B = B_K + i\Gamma_K/2$ is the complex binding energy. The real part of the \bar{K} optical potential V_{opt} is then given by

$$\text{Re } V_{\text{opt}} = \frac{m_K}{\mu} \left(\frac{1}{2} S - V - \frac{V^2}{2m_K} \right) , \quad (7)$$

where $S = g_{\sigma K} \sigma$ and $V = g_{\omega K} \omega_0$ are the scalar and vector potentials due to the σ and ω mean fields, respectively.

Since the RMF approach does not address the imaginary part of the potential, $\text{Im } V_{\text{opt}}$ was taken in a phenomenological $t\rho$ form, where its depth was fitted to the K^- atomic data [3]. Note that ρ in the present calculations is no longer a static nuclear density, but is a *dynamical* entity affected by the \bar{K} interacting with the nucleons via boson fields. The resulting compressed nuclear density leads to increased widths, particularly for deeply bound states. On the other hand, the phase space available for the decay products is reduced for deeply bound states, which will act to decrease the calculated widths. Thus, suppression factors multiplying $\text{Im } V_{\text{opt}}$ were introduced from phase-space considerations, taking into account the binding energy of the kaon for the initial decaying state, and assuming two-body final-state kinematics for the decay products. Two absorption channels were considered. In the first, Eq. (1), a $\bar{K}N$ initial state decays into a πY final state. The corresponding density-independent suppression factor is given by

$$f_1 = \frac{M_{01}^3}{M_1^3} \sqrt{\frac{[M_1^2 - (m_\pi + m_Y)^2][M_1^2 - (m_Y - m_\pi)^2]}{[M_{01}^2 - (m_\pi + m_Y)^2][M_{01}^2 - (m_Y - m_\pi)^2]}} \Theta(M_1 - m_\pi - m_Y) , \quad (8)$$

where $M_{01} = m_{\bar{K}} + m_N$, $M_1 = M_{01} - B_K$. In the second absorption channel, Eq. (2), a $\bar{K}NN$ initial state decays into a YN final state. The corresponding suppression factor is given by

$$f_2 = \frac{M_{02}^3}{M_2^3} \sqrt{\frac{[M_2^2 - (m_N + m_Y)^2][M_2^2 - (m_Y - m_N)^2]}{[M_{02}^2 - (m_N + m_Y)^2][M_{02}^2 - (m_Y - m_N)^2]}} \Theta(M_2 - m_Y - m_N) , \quad (9)$$

where $M_{02} = m_{\bar{K}} + 2m_N$, $M_2 = M_{02} - B_K$. Although multi-nucleon absorption modes are often modeled to have a power-law ρ^α ($\alpha > 1$) density dependence, our comprehensive K^- -atom fits [2,3] are satisfied with $\alpha \sim 1$. We therefore assume $\alpha = 1$ in this exploratory work also for this second absorption channel,* which means that f_2 too is independent of density. We comment below on the effect of a possible density dependence of f_2 , reflecting perhaps a ρ^2 dependence of the non-pionic decay mode (2) at high densities.

Since Σ final states dominate these channels [14] the hyperon Y was here taken as $Y = \Sigma$. Allowing Λ hyperons would foremost *add* conversion width to \bar{K} states bound in the region $B_K \sim 100 - 180$ MeV. For the combined suppression factor we assumed a mixture of 80% mesonic decay and 20% nonmesonic decay [14], i.e.

$$f = 0.8 f_1 + 0.2 f_2 . \quad (10)$$

This suppression factor is plotted as function of B_K in the upper part of Fig. 1, where a residual value of $f = 0.02$, when both f_1 and f_2 vanish, was assumed.

*a lucid theoretical discussion of this point, with allowance for $\alpha = 1$, is due to Koltun [22]

The coupled system of equations for nucleons and for the electromagnetic vector field A_0 , and for the mean fields σ and ω_0 , Eqs. (4,5) above, as well as the KG equation (6) for K^- were solved self-consistently using an iterative procedure. Obviously, the requirement of self-consistency is crucial for the proper evaluation of the dynamical effects of the \bar{K} on the nuclear core and vice versa. We note that self-consistency is not imposed here on the final-state hadrons which only enter through their *on-shell* masses used in the phase-space suppression factors given above. For the main $\pi\Sigma$ decay channel it is likely that the attraction provided by the pion within a dynamical calculation [15] is largely cancelled by the nuclear repulsion deduced phenomenologically for Σ hyperons [23–25].

III. RESULTS

The main objective of the present calculations of \bar{K} -nucleus bound states was to establish correlations between various observables such as the \bar{K} binding energy, width and macroscopic nuclear properties. In particular we aimed at covering a wide range of binding energies in order to evaluate widths of possible strongly bound \bar{K} states. Furthermore, in order to study effects of the nuclear polarization, we calculated rms radii and average densities of the nuclei involved and, in some cases, also single particle energies. Extensive calculations were made for ^{12}C and ^{16}O , nuclei that had been discussed earlier in the context of strongly bound \bar{K} states [6,11]. Additionally, more restricted calculations were made for ^{40}Ca and ^{208}Pb .

In a preliminary test we performed dynamical calculations for K^- *atomic* $1s$ states, which produced only negligibly small polarization effects, thus validating previous analyses of kaonic atom data. The empirical values $g_{\sigma K}^{(1)}$ and $g_{\omega K}^{(1)}$, as found from a fit to kaonic atom data [3], were therefore used as a starting point for calculations. A full dynamical calculation was then made for K^- *nuclear* states starting from the $t\rho$ imaginary potential obtained from the atomic fit, while entering dynamically in the iteration cycles the resulting nuclear density and the suppression factor f as defined by Eq.(10). This *dynamical* calculation nearly doubled, for the light nuclei here considered, the depth of the real part of the phenomenological *static* K^- -nucleus potential of Ref. [3] which is of the ‘deep’ variety, typically 150-200 MeV deep in the static calculation.

Since there is no preferred way of varying the depth of the real K^- -nucleus potential in order to produce different values of binding energies, we used two methods for scanning over binding energies. The first one, referred to below as the ‘RMF’ method, was to scale down successively $g_{\sigma K}$ from its initial value $g_{\sigma K}^{(1)}$ and, once it reached zero, to scale down $g_{\omega K}$ too from its initial value $g_{\omega K}^{(1)}$ until the K^- $1s$ state became unbound. As an alternative method we chose as a starting point values $g_{\sigma K}^{(2)}$ and $g_{\omega K}^{(2)}$ obtained from fits to kaonic atom data where the RMF-based real potential was joined at large radii by a ‘ $t\rho$ ’ expression, using for t the chiral $\bar{K}N$ amplitudes of Ramos and Oset [15]. This starting potential was of the ‘shallow’ variety [5], about 55 MeV deep in the static calculation. It is gratifying that the replacement of the chiral ‘ $t\rho$ ’ expression within the nucleus by the RMF model did not change the resulting \bar{K} -nuclear potential depth. We then increased the potential depth by scaling up $g_{\sigma K}$ from its initial value $g_{\sigma K}^{(2)}$, in order to achieve as deep binding as in the first set of calculations, while keeping $g_{\omega K}$ constant at its initial value $g_{\omega K}^{(2)}$. This second method will

be referred to below as the ‘chiral tail’ method. Note that in both methods ($j = 1, 2$) the starting values ($g_{\omega K}^{(j)}, g_{\sigma K}^{(j)}$) correspond to potentials that produce in the dynamical calculation good fits to the K^- atomic data, although $\text{Re } V_{\text{opt}}^{(j)}$ have vastly different depths. The good fits to the atomic data are inevitably lost once the coupling constants ($g_{\sigma K}$ in the procedure outlined above) are allowed to vary in order to scan over a wide range of binding energies and the associated widths.

Figure 1 shows, in its middle and lower parts, calculated widths Γ_{K^-} as function of the binding energy B_{K^-} for $1s$ states in $K^-{^{16}\text{O}}$ and $K^-{^{12}\text{C}}$, respectively. Open squares and solid circles are for the L and NL versions of the RMF model, respectively, both calculated using the ‘RMF’ method for scanning the binding energies. The crosses are for RMF-L, using the ‘chiral tail’ method for scanning the binding energies. It is clearly seen that the widths of the K^- nuclear state follow closely the dependence of the suppression factor on the binding energy and that, except for binding energies smaller than 50 MeV, the dependence of the width on the binding energy follows, for a given nucleus, almost a universal curve. We note that the widths calculated in the range $B_K \sim 100 - 200$ MeV assume values 40 ± 5 MeV, which are considerably larger than what the suppression factor of the upper part of the figure would suggest. This is largely related to the dynamical nature of the RMF calculation whereby the nuclear density is increased by the polarization effect of the K^- , as shown in the next figures. Furthermore, replacing ρ by ρ^2 for the density dependence of the non-pionic decay modes (2) is estimated to increase the above values of the width by 10 - 15 MeV. This estimate follows, again, from the increase of nuclear density with B_K noticed above. Switching on the $\pi\Lambda$ decay mode would increase further this estimate by 5-10 MeV in the range $B_K \sim 100 - 180$ MeV. We assert that the estimate $\Gamma_K = 40 \pm 5$ MeV in the range $B_K \sim 100 - 200$ MeV provides a reasonable lower bound on the width expected in any realistic calculation. A more detailed systematics is deferred to a subsequent regular report.

Figures 2 and 3 exhibit various nuclear properties for $1s$ states in $K^-{^{12}\text{C}}$ and $K^-{^{16}\text{O}}$, respectively. The top and middle parts show the calculated average nuclear density $\bar{\rho} = \frac{1}{A} \int \rho^2 d\mathbf{r}$ and the nuclear rms radius, respectively, and the lower parts show the $1s$ and $1p$ neutron single-particle energies E_n . The differences between the linear and non-linear models reflect the different nuclear compressibility and the somewhat different nuclear sizes obtained in the two models. Again, for K^- binding energy greater than 50 MeV the results are independent of the way the binding energy is being scanned. It is interesting to note that the increase in the nuclear rms radius of $K^-{^{16}\text{O}}$ for large values of B_{K^-} is the result of the reduced binding energy of the $1p_{1/2}$ state, due to the increased spin-orbit term. Note also that as B_{K^-} approaches zero we do *not* recover the values inherent in static calculations for the various nuclear entities because the coupling constants $g_{\sigma K}$ and $g_{\omega K}$, and the imaginary part of the potential, still assume nonzero values. The substantial increase of $\bar{\rho}$, the decrease of the nuclear rms radius, and the decrease of the $1s$ neutron single-particle energy, all point out to a significant polarization of the nuclear core by the $1s$ K^- . Finally, we note that in similar calculations for ^{40}Ca and ^{208}Pb the widths of the K^- nuclear state *vs.* its binding energy turned out to be similar in shape to the corresponding results for ^{12}C and ^{16}O , but the effects on the average density and the rms radius are negligibly small, as expected for heavier nuclei.

Table I shows several examples of the excited-state spectrum of K^- -nuclear states in the core of ^{16}O . The calculated widths of the excited states appear to follow the general trend

of widths for $1s$ states as shown in Fig. 1. The polarization of the nucleus as judged by the value of its average density $\bar{\rho}$ appears to diminish, the higher the K^- state is, in agreement with Fig. 3. We note the fairly large spacing between neighboring states: the effective $\hbar\omega$ is of order 100 MeV for the first spectrum, decreasing to 80 MeV and to 70 MeV in the second and third spectra, respectively, as the $1s$ binding is made lower. Static calculations give smaller spacings. Kishimoto et al. [11] have very recently suggested evidence from the measured neutron spectrum in the $^{16}\text{O}(K^-, n)$ reaction for a peak at $B_K \sim 90$ MeV which they interpreted as the $1p$ \bar{K} state, probably since a hint for a peak at $B_K \sim 130$ MeV is also suggested by the same spectrum. The results shown in Table I rule out such interpretation which would require $\hbar\omega \sim 40$ MeV, considerably less than our *dynamical* calculations produce. If the peak at $B_K \sim 90$ MeV were a $1p$ state, one should have expected the $1s$ state to be deeply bound, at $B_K \sim 200$ MeV where no signal has been observed. On the other hand, if this peak is a $1s$ state, then the relatively shallow $1p$ state would be expected too broad to be distinguished in the data.

IV. CONCLUSIONS

Binding energies and widths of deeply bound K^- nuclear states in ^{12}C and ^{16}O were calculated with the aim of establishing values of widths that could be expected for binding energies in the range of 100-200 MeV. The method chosen was to couple the K^- dynamically to the nucleus within the RMF approach, which is applicable throughout the periodic table, but which is disconnected from near-threshold $\bar{K}N$ phenomenology. Negligible polarization effects were found for *atomic* states, which confirms the optical-potential phenomenology of kaonic atoms as a valid starting point for the present study. Substantial polarization of the core nucleus was found in these light nuclei for deeply bound \bar{K} nuclear states. Almost universal dependence of antikaon widths on its binding energy was found, for a given nucleus, suggesting that the details of how the calculated binding energy is varied over the desired range of values is largely immaterial. The widths are mostly determined by the phase-space suppression factors on top of the increase provided by the density of the compressed nuclei. The present results already provide useful guidance for the interpretation of recent experimental results [11] by placing a lower limit $\Gamma_K \sim 35 - 40$ MeV on \bar{K} states in ^{16}O bound in the range $B_K \sim 100 - 200$ MeV. For lighter nuclear targets such as ^4He , where the RMF approach becomes unreliable but where nuclear polarization effects are found larger using few-body calculational methods [7,8], we anticipate larger widths for \bar{K} deeply bound states, if such states do exist [10].

This work was supported in part by the GA AVCR grant IAA1048305 and by the Israel Science Foundation grant 131/01.

REFERENCES

- [1] C.J. Batty, E. Friedman, A. Gal, Phys. Rep. 287 (1997) 385.
- [2] E. Friedman, A. Gal, C.J. Batty, Phys. Lett. B 308 (1993) 6; Nucl. Phys. A 579 (1994) 518.
- [3] E. Friedman, A. Gal, J. Mareš, A. Cieplý, Phys. Rev. C 60 (1999) 024314.
- [4] A. Baca, C. García-Recio, J. Nieves, Nucl. Phys. A 673 (2000) 335.
- [5] A. Cieplý, E. Friedman, A. Gal, J. Mareš, Nucl. Phys. A 696 (2001) 173.
- [6] T. Kishimoto, Phys. Rev. Lett. 83 (1999) 4701.
- [7] Y. Akaishi, T. Yamazaki, Phys. Rev. C 65 (2002) 044005.
- [8] A. Doté, H. Horiuchi, Y. Akaishi, T. Yamazaki, Phys. Lett. B 590 (2004) 51; Phys. Rev. C 70 (2004) 044313.
- [9] M. Iwasaki, et al., arXiv:nucl-ex/0310018; T. Suzuki, et al., to be published in the proceedings of HYP03 in Nucl. Phys. A (2005).
- [10] T. Suzuki, et al., Phys. Lett. B 597 (2004) 263.
- [11] T. Kishimoto, et al., to be published in the proceedings of HYP03 in Nucl. Phys. A (2005).
- [12] KEK-PS proposals E548, E549 (2003) scheduled for Spring 2005.
- [13] T. Yamazaki, Y. Akaishi, Phys. Lett. B 535 (2002) 70.
- [14] C. Vander Velde-Wilquet, J. Sacton, J.H. Wickens, D.N. Tovee, D.H. Davis, Nuovo Cimento A 39 (1977) 538.
- [15] A. Ramos, E. Oset, Nucl. Phys. A 671 (2000) 481.
- [16] J. Schaffner, A. Gal, I.N. Mishustin, H. Stöcker, W. Greiner, Phys. Lett. B 334 (1994) 268.
- [17] J. Schaffner, I.N. Mishustin, Phys. Rev. C 53 (1996) 1416.
- [18] T. Bürvenich, I.N. Mishustin, L.M. Satarov, J.A. Maruhn, H. Stöcker, W. Greiner, Phys. Lett. B 542 (2002) 261.
- [19] I.N. Mishustin, L.M. Satarov, T.J. Bürvenich, H. Stöcker, W. Greiner, submitted to Phys. Rev. C [arXiv:nucl-th/0404026].
- [20] C.J. Horowitz, B.D. Serot, Nucl. Phys. A 368 (1981) 503.
- [21] M.M. Sharma, M.A. Nagarajan, P. Ring, Phys. Lett. B 312 (1993) 377.
- [22] D.S. Koltun in *Meson-Nuclear Physics 1979*, ed. E.V. Hungerford III, AIP Conf. Proc. 54 (AIP, New York, 1979) 87.
- [23] J. Mareš, E. Friedman, A. Gal, B.K. Jennings, Nucl. Phys. A 594 (1995) 311.
- [24] H. Noumi, et al., Phys. Rev. Lett. 89 (2002) 072301; 90 (2003) 049902(E).
- [25] P.K. Saha, et al., Phys. Rev. C 70 (2004) 044613.

TABLES

TABLE I. K^- bound-state spectra in $_{K^-}^{16}\text{O}$ calculated for several RMF (NL) Lagrangians specified by different coupling-constant ratios $\alpha_\sigma = g_{\sigma K}/g_{\sigma K}^{(1)}$ and $\alpha_\omega = g_{\omega K}/g_{\omega K}^{(1)}$. The static average density for ^{16}O is $\bar{\rho} = 0.100 \text{ fm}^{-3}$.

α_σ	α_ω	nl	B_{K^-} (MeV)	Γ_{K^-} (MeV)	$\bar{\rho}$ (fm $^{-3}$)
0.45	1	1s	196.1	35.0	0.133
		1p	82.2	83.0	0.127
		2s	3.7	89.9	0.111
0.05	1	1s	133.9	38.7	0.127
		1p	50.6	119.0	0.120
0	0.85	1s	90.2	64.2	0.121
		1p	23.8	124.5	0.115

FIGURES

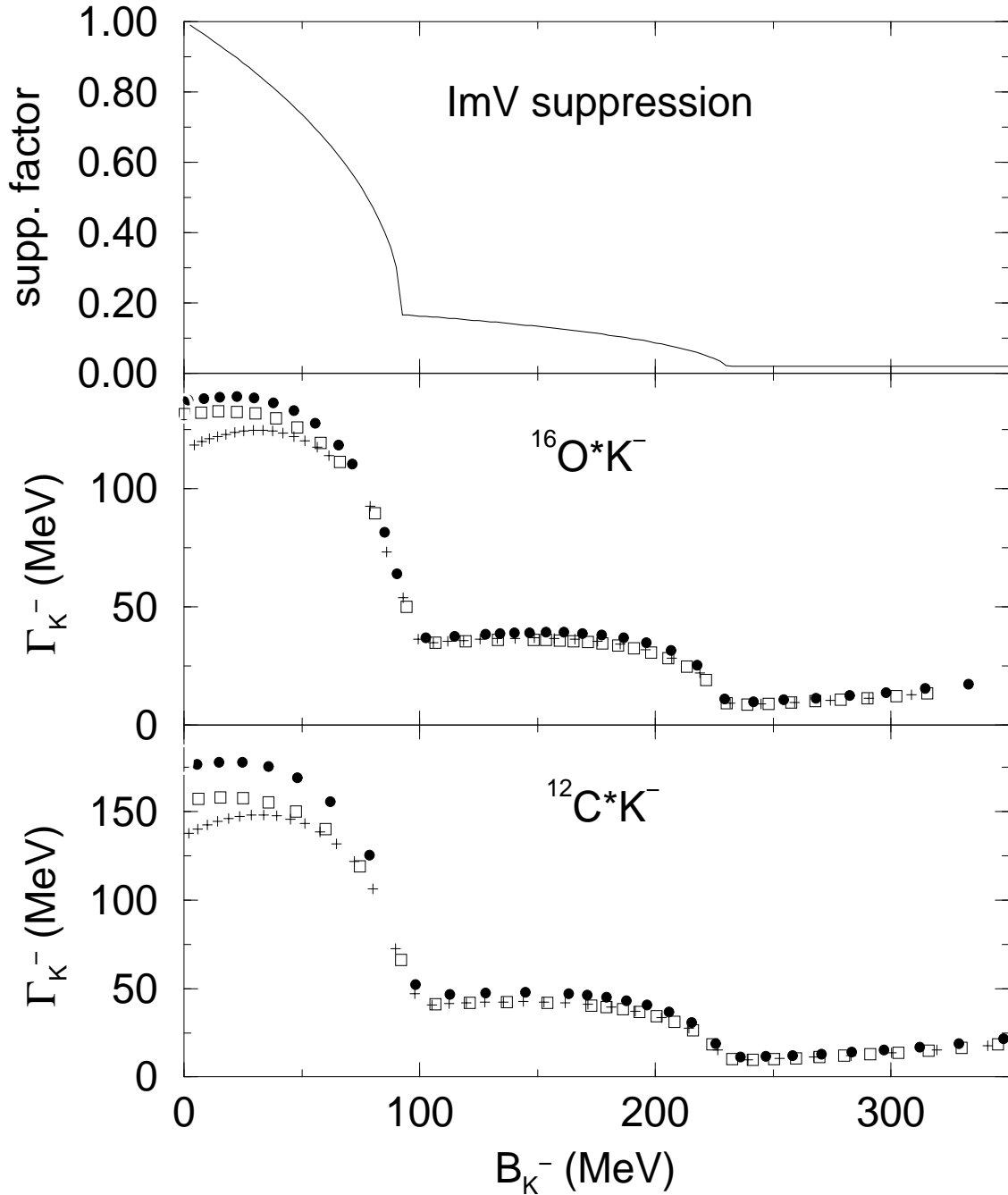


FIG. 1. Phase-space suppression factor for the imaginary potential (top), and widths of the $1s$ K^- -nuclear state (middle: in ^{16}O , bottom: in ^{12}C) as function of the K^- binding energy (see text for symbols).

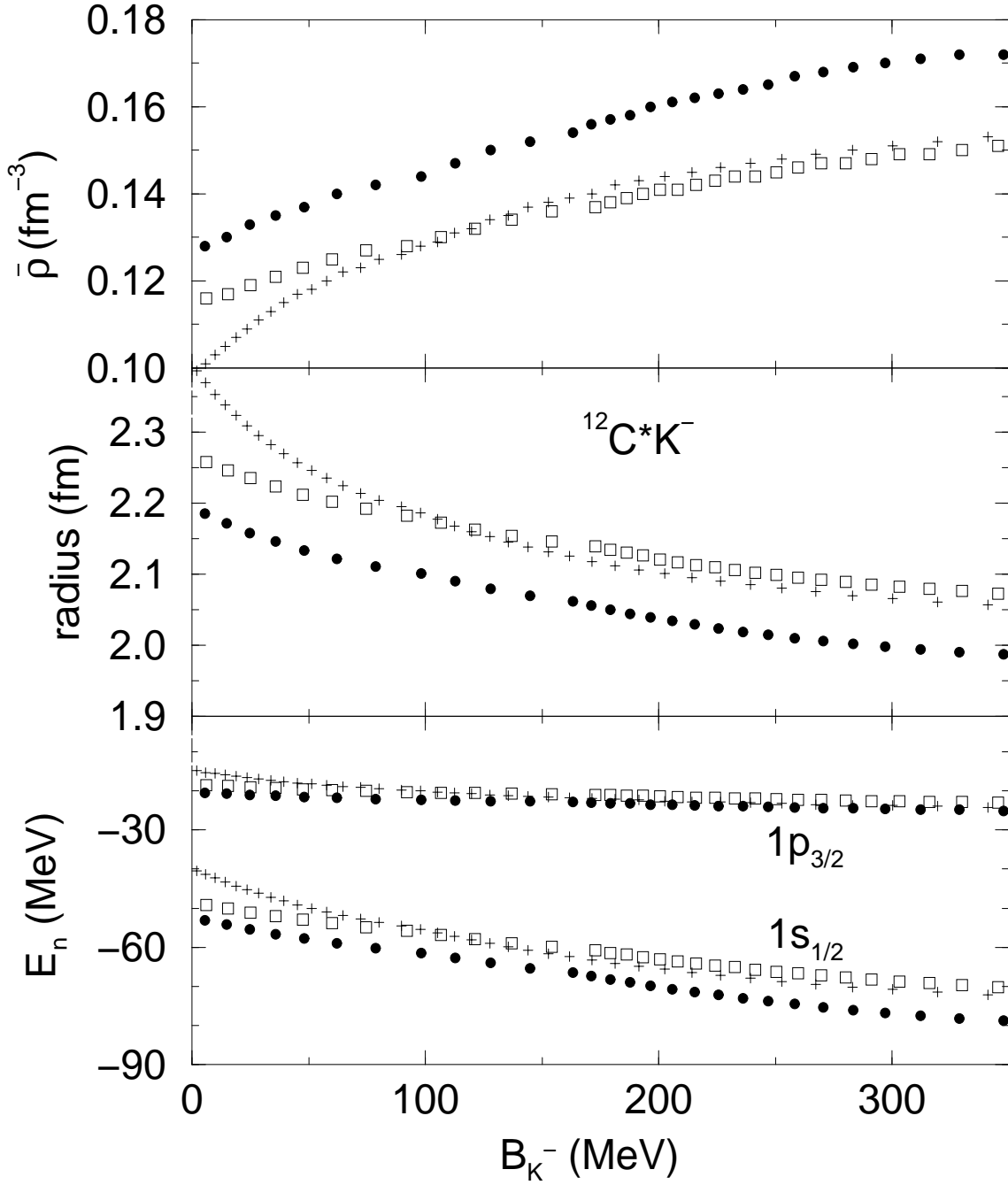


FIG. 2. Average nuclear density, nuclear rms radius and neutron single-particle energies for $K^-^{12}\text{C}$. Symbols are as in Fig. 1.

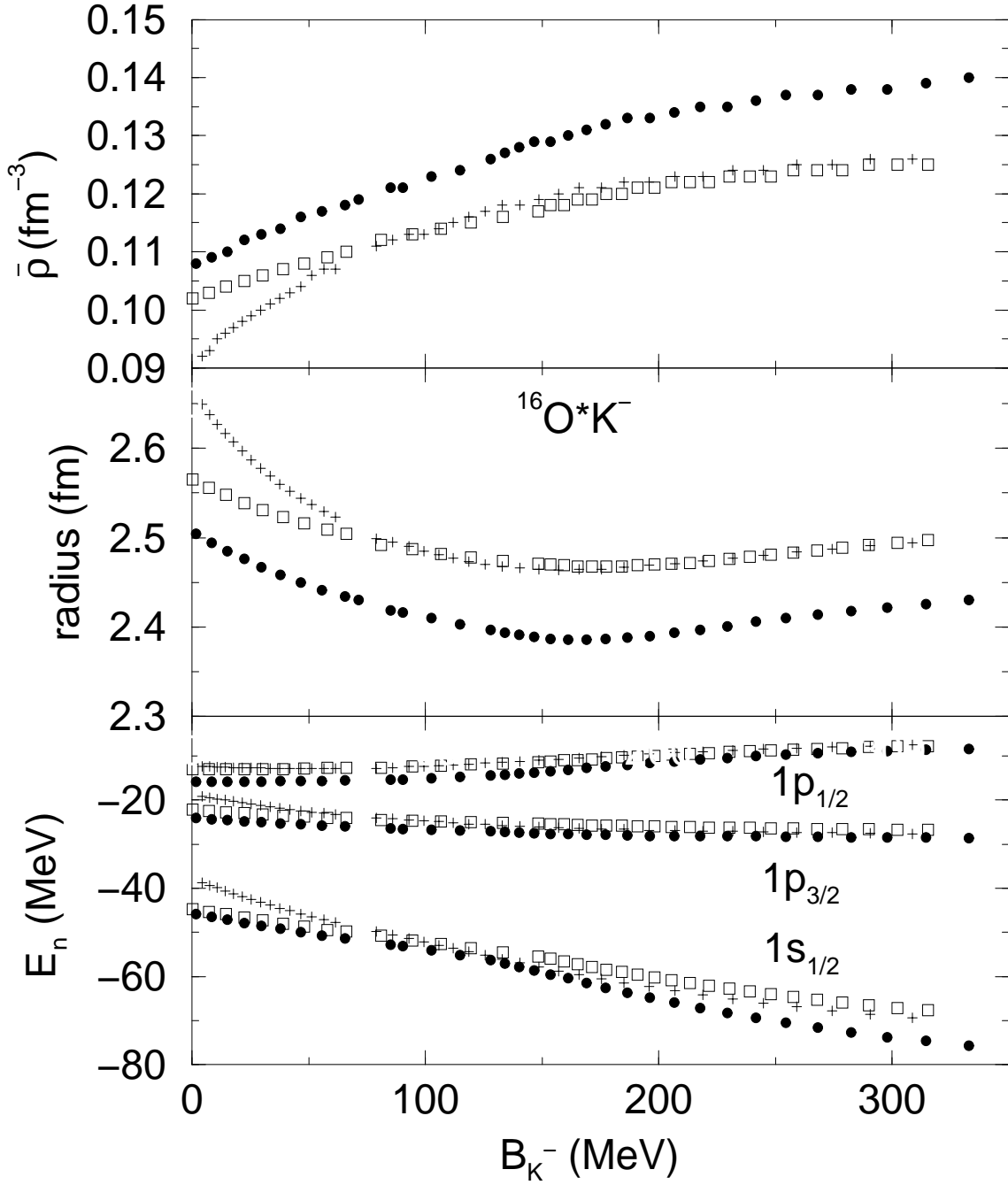


FIG. 3. Average nuclear density, nuclear rms radius and neutron single-particle energies for $^{16}\text{O}^* \text{K}^-$. Symbols are as in Fig. 1.